Multi-institutional Collaborations for Improving Deep Learning-based Magnetic Resonance Image Reconstruction Using Federated Learning

Pengfei Guo, Puyang Wang, Jinyuan Zhou, Shanshan Jiang, Vishal M. Patel

CVPR 2021

Johns Hopkins University

Outline

- Introduction
- Method
- Results
- Discussions

Introduction

The forward model for MR is as follows:

$$y = Ax + e \quad (1)$$

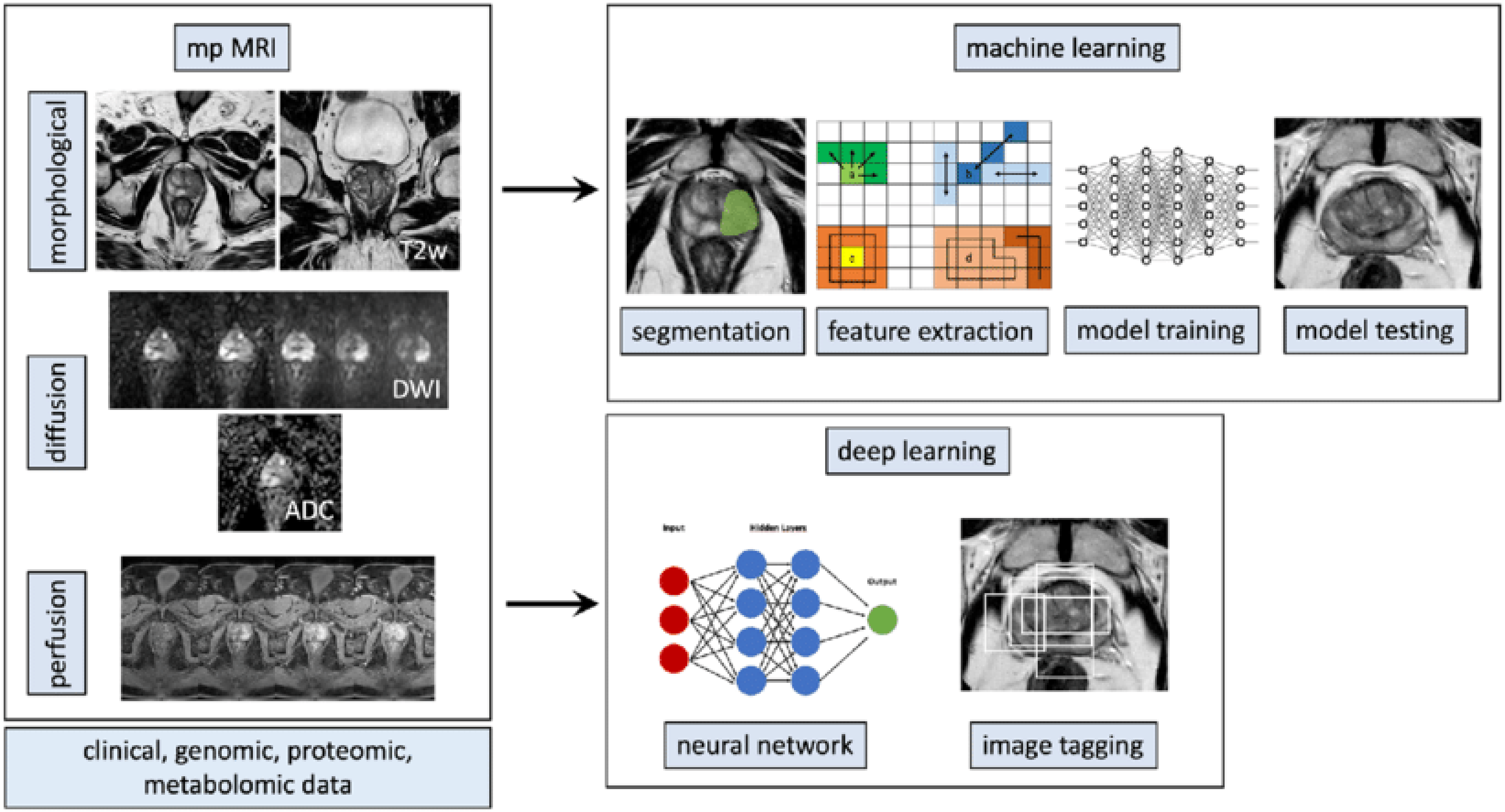

Deep learning shows great power in aspect of MR imaging

Introduction

Main challenges:

(1) difficult to collect and share large datasets due to the high cost of acquisition and medical data privacy regulations;
solution: proposed a federated learning (FL) based solution in which we take advantage of the MR data available at different institutions while preserving patients' privacy.

(2) the generalizability of models trained with the FL setting can still be suboptimal due to domain shift with the data collected at multiple institutions;
solution: proposed a cross-site modeling for MR image reconstruction in which the learned intermediate latent features among different source sites are aligned with the distribution of the latent features at the target site.

Outline

- Introduction
- Method
- Results
- Discussions

Federated Learning

- **Federated learning is a decentralized learning framework which allows multiple institutions to collaboratively learn a shared machine learning model without sharing their local training data**

  FL training process consists of the following steps:
  (1) All institutions locally compute gradients and send locally trained network parameters to the server.
  (2) The server performs aggregation over the uploaded parameters from K institutions.
  (3) The server broadcasts the aggregated parameters to K institutions.
  (4) All institutions update their respective models with aggregate parameters and test the performance of the updated models.

- **The institutions collaboratively learn a machine learning model with the help of a central cloud server. Then, a global optimal learned model can be obtained.**

FL-MR framework

The basic MR reconstruction model can be expressed as

$$\boldsymbol{x} = \boldsymbol{F}^{-1}(\boldsymbol{F}_d\boldsymbol{y} + \boldsymbol{\epsilon}), \quad \boldsymbol{x}, \boldsymbol{y} \in \boldsymbol{C}^N \tag{1}$$

where $\boldsymbol{x}$ denotes the observed undersampled image, $\boldsymbol{y}$ is the fully-sampled image, and $\boldsymbol{\epsilon}$ denotes noise. Here, $\boldsymbol{F}$ and $\boldsymbol{F}^{-1}$ denote the Fourier transform matrix and its inverse, respectively. $\boldsymbol{F}_d$ represents the undersampling Fourier encoding matrix.

FL-MR framework

Let $D^1, \ldots, D^K$ denote the MR image reconstruction datasets from *K* different institutions. Each local dataset D^k contains pairs of under-sampled and fully-sampled images. At each institution, a local model is trained using its own data by iteratively minimizing the following loss

$$L_{recon} = \sum_{(x,y)\in D^k} \left\| G^k(x) - y \right\|_1 \quad (2)$$

where G^k corresponds to the local model at site *k* and is parameterized by ΘG^k. $G^k(x)$ corresponds to the reconstructed image y. After optimization with several local epochs (i.e. P epochs)

$$\Theta_{G^k}^{(p+1)} \leftarrow \Theta_{G^k}^{(p)} - \gamma \nabla L_{recon}, \quad (3)$$

Limitation 1: a local model is trained using its own data, it introduces a bias and does not generalize well to MR images from another institutions

FL-MR framework

Without accessing private data in each site, the proposed FL-MR method leverages a central server to utilize the information from other institutions by aggregating local model updates

$$\Theta_G^{(q)} = \frac{1}{K}\sum_{k=1}^{K} \Theta_{G^k}^{(q)} \quad (4)$$

Algorithm 1: FL-based MRI Reconstruction

Input: $\mathcal{D} = \{\mathcal{D}^1, \mathcal{D}^2, \ldots, \mathcal{D}^K\}$, datasets from K institution; P, the number of local epoches; Q, the number of global epoches; γ, learning rate; $G^1, G^2, \ldots, G^K$, local models parameterized by $\Theta_{G^1}, \Theta_{G^2}, \ldots, \Theta_{G^K}$; G, the global model parameterized by Θ_G.

Output: well-trained global model G

```
▷ parameters initialization;
for q = 1 to Q do
    for k = 1 to K in parallel do
        ▷ deploy weights to local model;
        for p = 1 to P do
            ▷ compute reconstruction loss L_recon
              with Eq. 2 and update parameters Θ_{G^k};
        end
        ▷ upload weights to server;
    end
    ▷ update global model with Eq. 4;
end
return Θ_G^Q
```

FL-MR framework

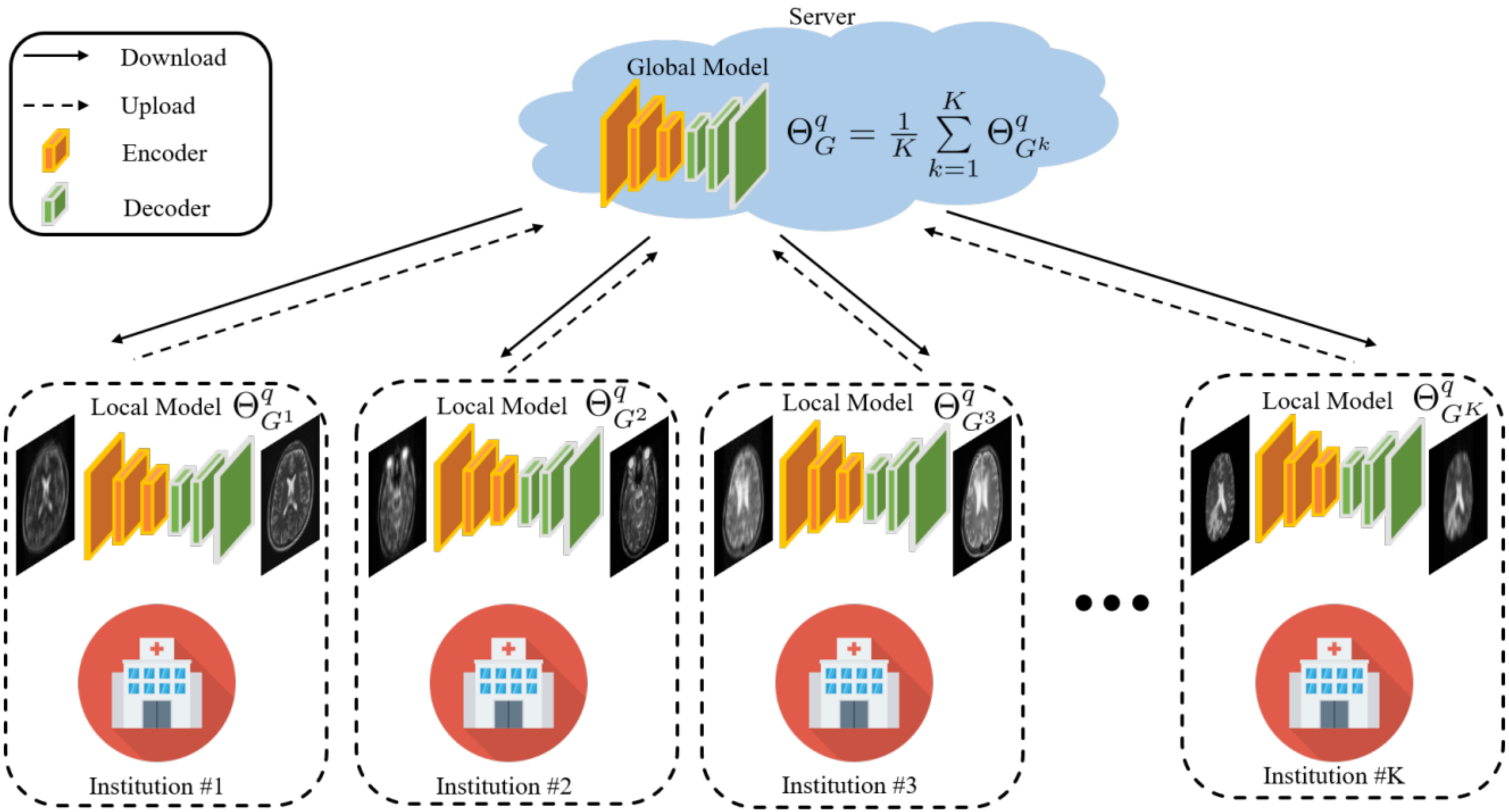

Figure 1. An overview of the proposed FL-MR framework.

FL-MRCM

- **LIMITATION 2: Domain shift among datasets inevitably degrades the performance of machine learning models, FL-MR with Cross-site Modeling (FL-MRCM) was proposed.**

- **For a source site D_s^k, they leverage the encoder part of the reconstruction networks (E_s^k) to project input onto the latent space z_s^k. Similarly, we can obtain z_t for the target site D_t . For each $\{D_s^k, D_t\}$ source-target domain pair, we introduce an adversarial domain identifier C^k to align the latent space distribution between the source domain and the target domain.**

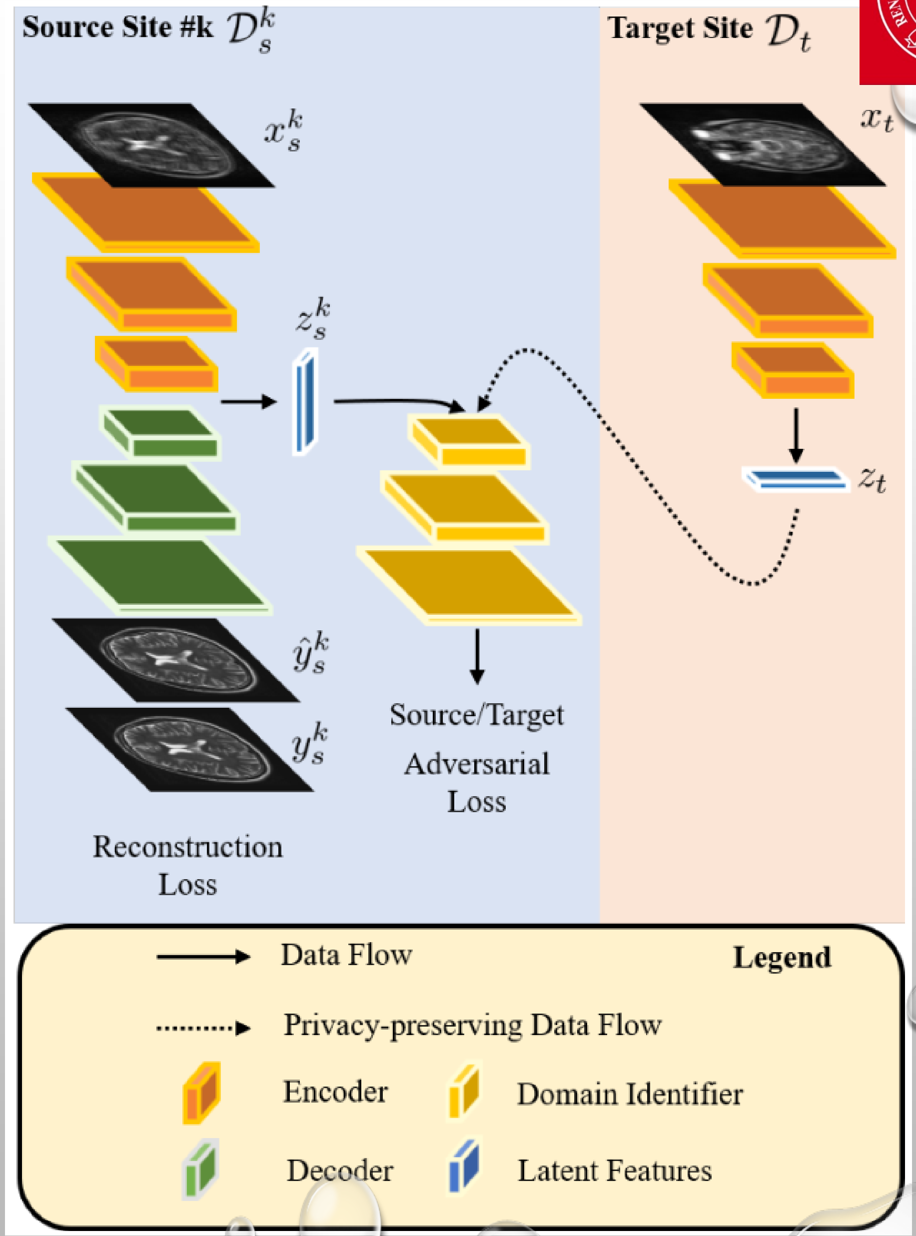

An overview of the proposed FL-MR framework with cross-site modeling in a source site.

FL-MRCM

Input: $\mathcal{D}_s = \{\mathcal{D}_s^1, \mathcal{D}_s^2, \ldots, \mathcal{D}_s^K\}$, data from the K source institutions; $\mathcal{D}_t$, data from the target institution; P, the number of local epoches; Q, the number of global epoches; γ, learning rate; $\Theta_{G_s^1}, \ldots, \Theta_{G_s^K}$, parameters of the local models in the source sites; $\Theta_{\mathcal{C}^1}, \ldots, \Theta_{\mathcal{C}^K}$, domain identifiers; Θ_G, the global model; Θ_{E_t}, the encoder part of G in the target site.

▷ parameters initialization

for q = *0 to* Q **do**

    for k = *0 to* K ***in parallel*** **do**

        ▷ deploy weights to local model

        for p = *0 to* P **do**

            Reconstruction:

            ▷ compute reconstruction loss $\mathcal{L}_{\text{recon}}$ using Eq. 2

            Cross-site Modeling:

            ▷ compute adverisal loss $\mathcal{L}_{\text{adv}\mathcal{C}^k}$ and $\mathcal{L}_{\text{adv}E_s^k}$ using Eq. 5 and Eq. 6

            ▷ compute the total loss using Eq. 7 and update $\Theta_{G_s^k}$, $\Theta_{\mathcal{C}^k}$, and Θ_{E_t}

        end

        ▷ upload weights to the central server

    end

    ▷ update the global model using Eq. 4

end

$$\mathcal{L}_{\text{adv}\mathcal{C}^k} = -\mathbb{E}_{x_s^k \sim \mathcal{D}_s^k}[\log \mathcal{C}^k(z_s^k)] - \mathbb{E}_{x_t \sim \mathcal{D}_t}[\log(1 - \mathcal{C}^k(z_t))], \tag{5}$$

where $z_s^k = E_s^k(x_s^k)$ and $z_t = E_t(x_t)$. The loss function for encoders can be defined as follows

$$\mathcal{L}_{\text{adv}E^k} = -\mathbb{E}_{x_s^k \sim \mathcal{D}_s^k}[\log \mathcal{C}^k(z_s^k)] - \mathbb{E}_{x_t \sim \mathcal{D}_t}[\log \mathcal{C}^k(z_t)]. \tag{6}$$

The overall loss function used for training the k-th source site with data $\mathcal{D}_s^k$ consists of the reconstruction and adversarial losses. It is defined as follows

$$\mathcal{L}_{\mathcal{D}_s^k} = \mathcal{L}_{\text{recon}} + \lambda_{\text{adv}}(\mathcal{L}_{\text{adv}\mathcal{C}^k} + \mathcal{L}_{\text{adv}E^k}), \tag{7}$$

Outline

- Introduction
- Method
- Results
- Discussions

Experiments conditions

Network details: The U-Net style encoder-decoder architecture for the reconstruction networks. λ_{adv} is set equal to 1. Acceleration factor (AF) is set equal to 4. The network is trained using the Adam optimizer with the following hyperparameters: constant learning rate of 1×10^{-4} for the first 40 global epochs then 1×10^{-5} for the last global 10 epochs; 50 maximum global epochs; 2 maximum local epochs; batch size of 16. During training, the cross- sectional images are zero-padded or cropped to the size of 256x256.

Dataset1--fastMRI (F for short): T1-weighted images corresponding to 3443 subjects are used for conducting experiments. In particular, data from 2583 subjects are used for training and remaining data from 860 subjects are used for testing. In addition, T2-weighted images from 3832 subjects are also used, where data from 2874 subjects are used for training and data from 958 subjects are used for testing.

Dataset2--HPKS (H for short): This dataset is collected from post-treatment patients with malignant glioma. T1 and T2-weighted images from 144 subjects are analyzed, where 116 subjects' data are used for training and 28 subjects' data are used for testing.

Dataset3--IXI (I for short): T1-weighted images from 581 subjects are used, where 436, 55 and 90 subjects' data are used for training, validation and testing. T2-weighted images from 578 subjects are also analyzed, where 434, 55 and 89 subjects' data are used for training, validation and testing. For each subject, there are approximately 150 and 130 axial cross-sectional images.

Dataset4--BraTS] (B for short): T1 and T2-weighted images from 494 subjects are used, where 369 and 125 subjects' data are used for training and testing. For each subject, approximately 120 axial cross-sectional images that contain brain tissues are provided for both MR sequences.

Experiments conditions

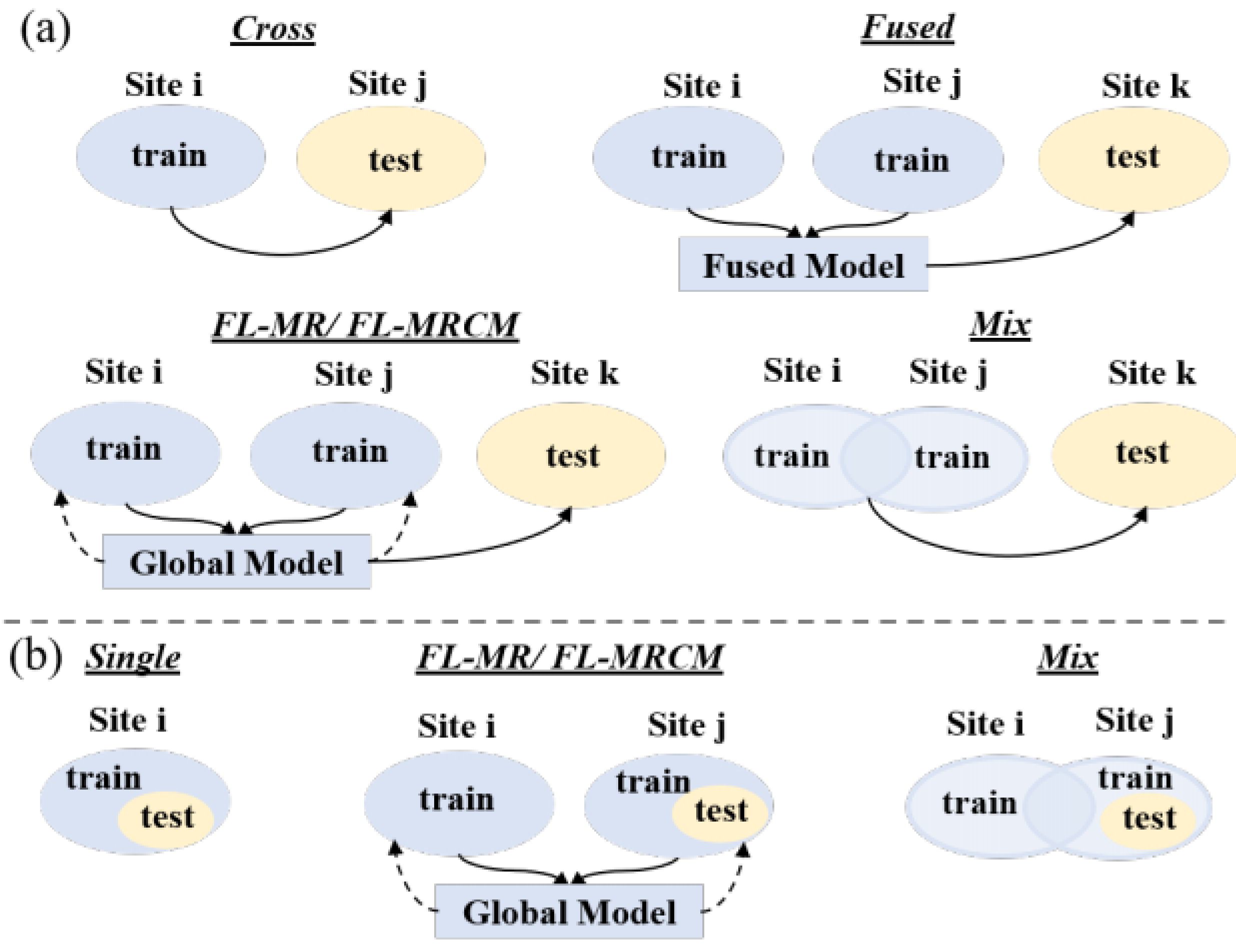

Figure 3. The schematic of different training strategies in (a) Scenario 1, and (b) Scenario 2. Note that for FL-MRCM, the source sites are the institutions that provide training data and the target site is the institution that provides testing data.

Experiments results (Scenario 1)

Table 1. Quantitative comparison with models trained by different strategies in Scenario 1.

Methods	Data Centers (Institutions)		T_1-weighted				T_2-weighted			
	Train	Test	SSIM	PSNR	Average SSIM	Average PSNR	SSIM	PSNR	Average SSIM	Average PSNR
Cross	F	B	0.9016	34.65	0.7907	30.02	0.9003	33.09	0.8296	29.51
	H	B	0.6670	29.12			0.8222	31.06		
	I	B	0.8795	33.76			0.8610	31.36		
	B	F	0.7694	28.61			0.7851	27.63		
	H	F	0.8571	31.82			0.8682	29.04		
	I	F	0.8417	31.18			0.8921	30.08		
	B	H	0.5188	25.07			0.5898	26.28		
	F	H	0.8402	28.52			0.8842	30.09		
	I	H	0.6281	27.09			0.8583	29.45		
	B	I	0.8785	30.10			0.7423	27.75		
	F	I	0.9102	31.16			0.8917	29.57		
	H	I	0.7968	29.16			0.8598	28.74		
Fused	F, H, I	B	0.8672	33.98	0.8223	31.27	0.8696	32.73	0.8264	30.17
	B, H, I	F	0.8557	32.03			0.8524	29.19		
	B, F, I	H	0.6615	27.87			0.7394	29.28		
	B, F, H	I	0.9047	31.22			0.8441	29.47		
FL-MR	F, H, I	B	0.9452	35.59	0.8976	32.09	0.916	33.76	0.8997	31.49
	B, H, I	F	0.9099	33.15			0.8991	30.86		
	B, F, I	H	0.8249	28.49			0.8874	31.02		
	B, F, H	I	0.9103	31.11			0.8962	30.32		
FL-MRCM	F, H, I	B	**0.9504**	**35.93**	**0.9108**	**32.51**	**0.9275**	**33.96**	**0.9113**	**31.77**
	B, H, I	F	**0.9149**	**33.31**			**0.9139**	**31.31**		
	B, F, I	H	**0.8581**	**29.24**			**0.8978**	**31.35**		
	B, F, H	I	**0.9197**	**31.54**			**0.9058**	**30.47**		
Mix (Upper Bound)	F, H, I	B	0.9589	36.68	0.9182	32.96	0.9464	34.58	0.9260	32.44
	B, H, I	F	0.9222	33.79			0.9239	31.89		
	B, F, I	H	0.8630	29.19			0.9168	32.14		
	B, F, H	I	0.9286	32.19			0.9169	31.14		

In addition, the **Mix** trained with data from all available data centers, this case compromises subjects' privacy from other institutions, so we treat it as an upper bound.

Experiments results (Scenario 1)

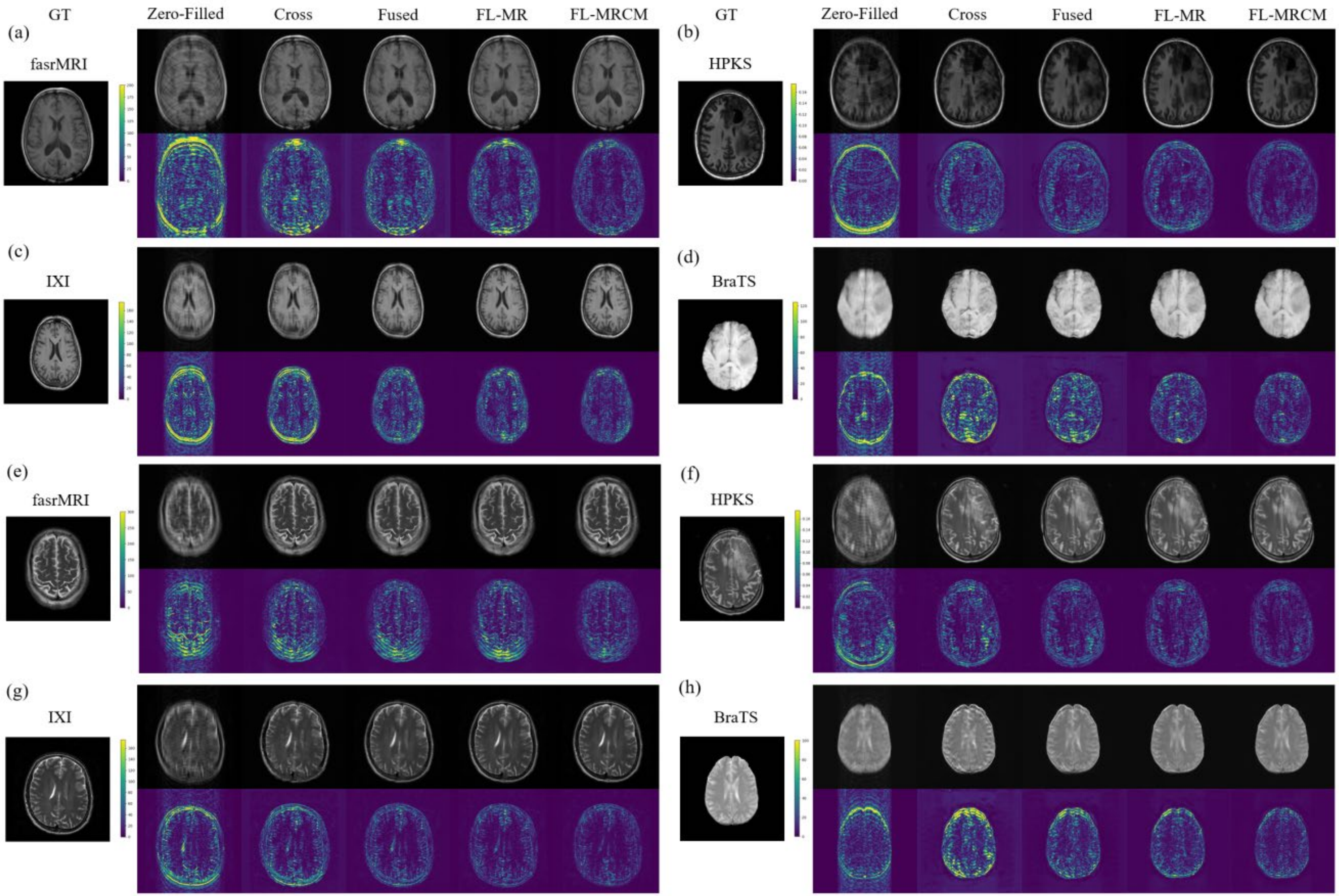

FL-MRCM method yields reconstructed images with remarkable visual similarity to the reference images compared to the other alternatives.

Experiments results (Scenario 2)

Table 2. Quantitative comparison with models trained by different strategies in Scenario 2.

Methods	Data Centers (Institutions)		T_1-weighted				T_2-weighted			
	Tain	Test	SSIM	PSRN	Average		SSIM	PSNR	Average	
					SSIM	PSNR			SSIM	PSNR
Single	B	B	0.9660	37.30	0.9351	33.81	0.9558	34.90	0.9278	32.35
	F	F	0.9494	35.45			0.9404	32.43		
	H	H	0.8855	29.67			0.9001	31.29		
	I	I	0.9396	32.80			0.9151	30.79		
FL-MR	B, F, H, I	B	0.9662	37.37	0.9294	33.92	0.9482	35.34	0.9238	32.64
		F	0.9404	35.25			0.9306	32.19		
		H	0.8732	30.03			0.9021	31.74		
		I	0.9379	33.03			0.9145	31.29		
FL-MRCM	B, F, H, I	B	0.9676	37.57	**0.9381**	**34.14**	0.9630	35.85	**0.9373**	**33.13**
		F	0.9475	35.57			0.9385	32.69		
		H	0.8940	30.27			0.9232	32.44		
		I	0.9432	33.13			0.9244	31.54		
Mix (Upper Bound)	B, F, H, I	B	0.9698	37.62	0.9440	34.35	0.9655	35.83	0.9398	33.14
		F	0.9558	36.15			0.9435	32.82		
		H	0.9047	30.57			0.9236	32.47		
		I	0.9454	33.08			0.9266	31.44		

Experiments results (Scenario 2)

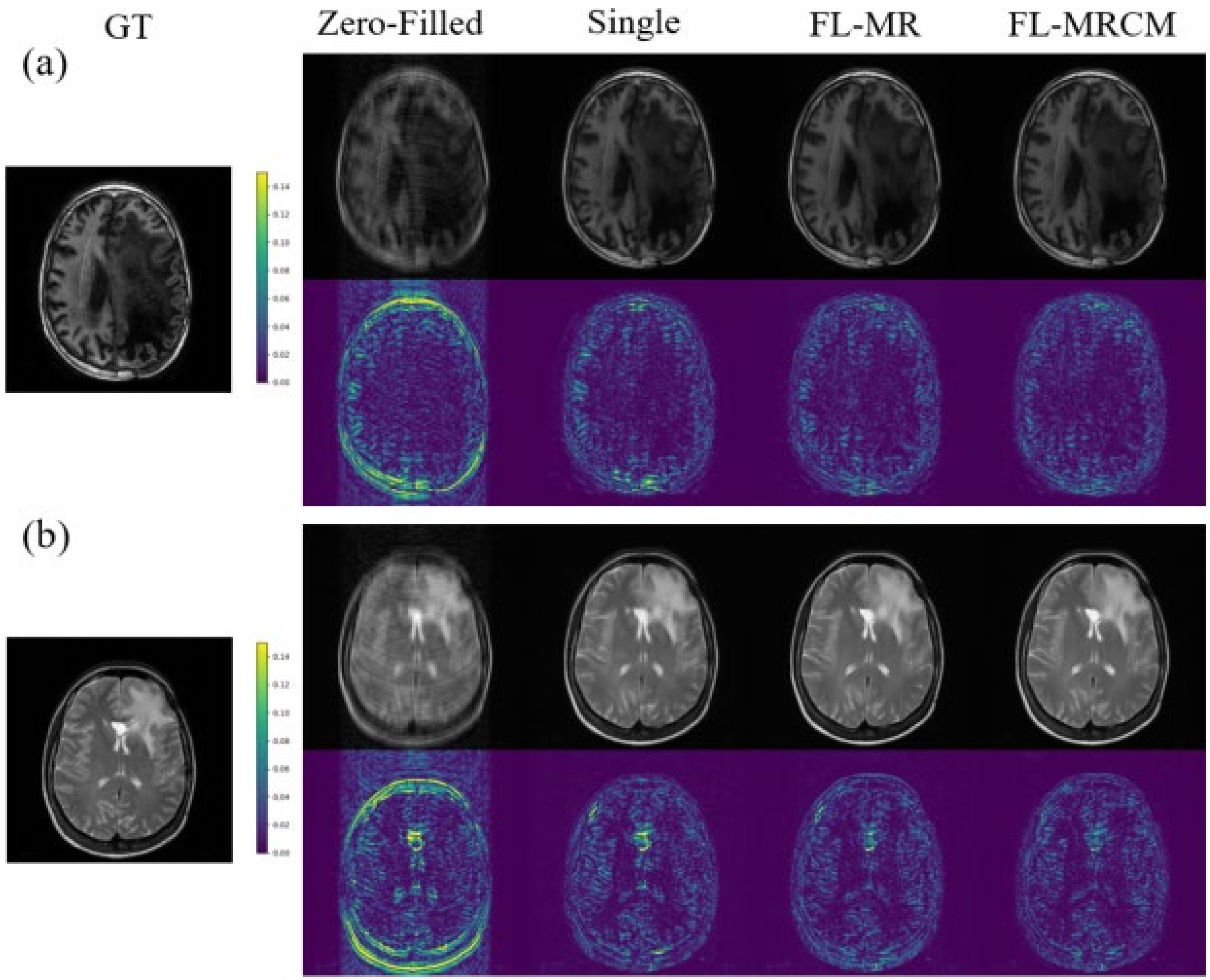

Qualitative results and error maps corresponding to different methods in Scenario 2 on HPKS. (a) T1- weighted, and (b) T2-weighted images

Experiments results: Ablation study

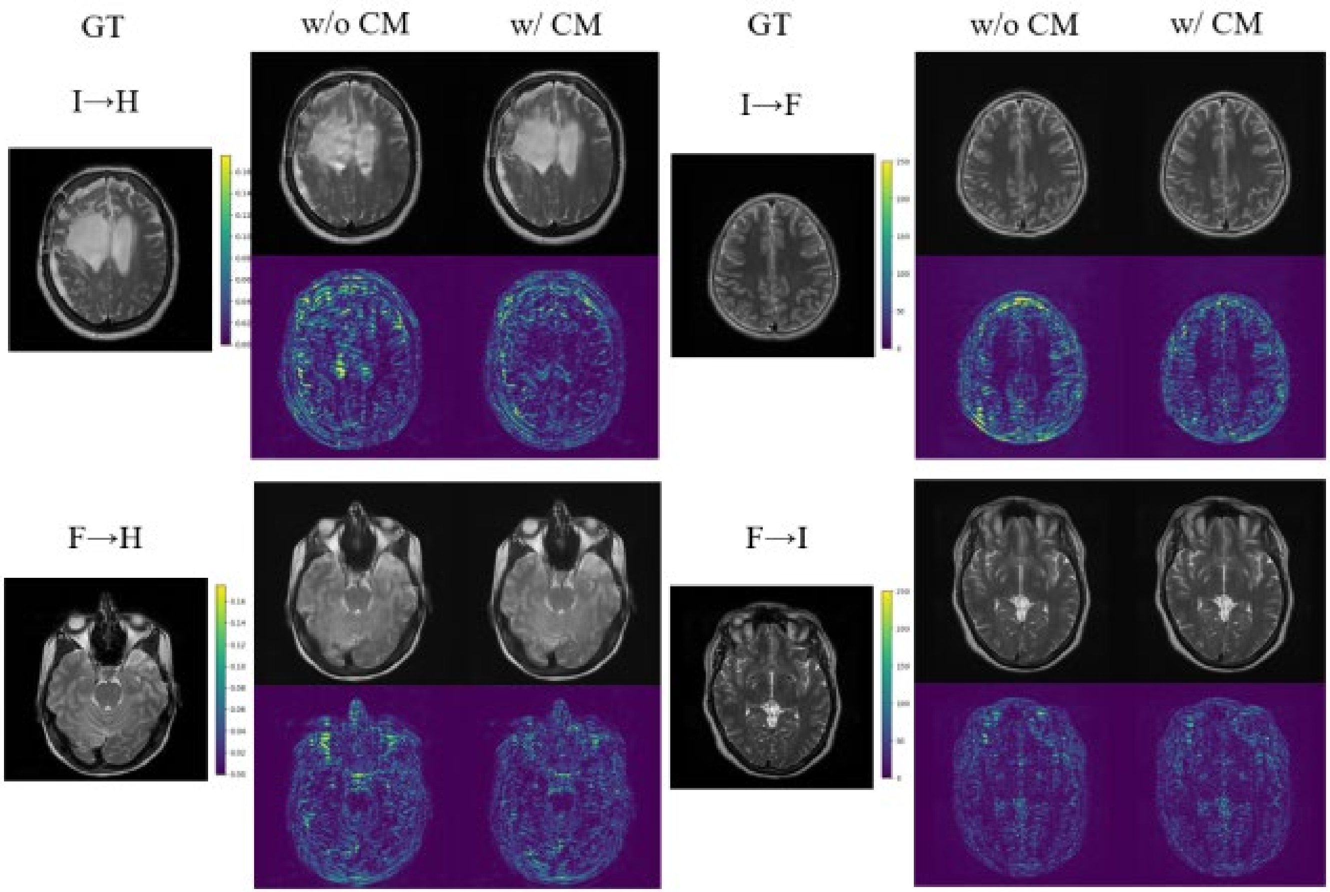

Qualitative comparisons and error maps on the T2 weighted images using cross-site modeling (CM). I→H represents the results from the model trained on I and tested on H, etc

Experiments results: Ablation study

Data Centers (Institutions)		w/o Cross-site Modeling				w/ Cross-site Modeling			
		SSIM	PSNR	Average		SSIM	PSNR	Average	
Train	Test			SSIM	PSNR			SSIM	PSNR
B	F	0.7851	27.63	0.7057	27.22	0.7914	27.85	**0.7525**	**27.32**
B	H	0.5898	26.28			0.6806	26.08		
B	I	0.7423	27.75			0.7856	28.03		
F	B	0.9003	33.09	0.8921	30.92	0.9139	33.84	**0.9027**	**31.58**
F	H	0.8842	30.09			0.8936	30.75		
F	I	0.8917	29.57			0.9004	30.14		
H	B	0.8222	31.06	0.8501	29.61	0.8391	31.54	**0.8582**	**30.07**
H	F	0.8682	29.04			0.8646	29.36		
H	I	0.8598	28.74			0.8709	29.31		
I	B	0.8610	31.36	0.8738	30.30	0.8946	32.11	**0.8949**	**31.06**
I	F	0.8921	30.08			0.9065	30.80		
I	H	0.8583	29.45			0.8837	30.26		

Quantitative ablation study of the proposed cross-site modeling on the T2-weighted images. For experiments with cross-site modeling, the target site is the institution that provides the test data.

Outline

- Introduction
- Method
- Results
- Discussions

Discussions

Conclusions:

(1) FL-based framework to leverage multi-institutional data for the MR image reconstruction task in a privacy-preserving manner;
(2) A cross-site modeling approach that provides the supervision to align the latent space distribution between the source domain and the target domain in each local entity without directly sharing the data;
(3) The benefits of multi-institutional collaborations under the FL-based framework in MR image reconstruction task.

Discussions:

(1) FL can be also extended to CT imaging to solve the current challenges;
(2) More complex FL models may be benefit to image reconstruction.